Atmospheric chemistry of hydrofluoroethers: Reaction of a series of hydrofluoroethers with OH radicals and Cl atoms, atmospheric lifetimes, and global warming potentials

Supporting Information

*Nathan Oyaro, Stig R. Sellevåg and Claus J. Nielsen**

Department of Chemistry, University of Oslo, P.O.Box 1033 Blindern, N-0315 Oslo, Norway

E-mail: claus.nielsen@kjemi.uio.no

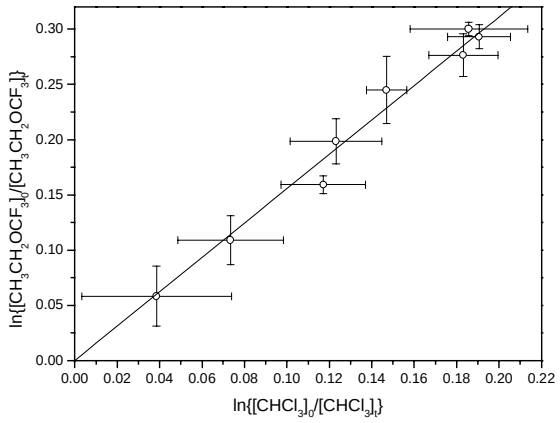

Fig. S1 Decay of $CH_3CH_2OCF_3$ versus $CHCl_3$ in the presence of OH radicals at 298 ± 2 K. 8 Data points give a relative reaction rate k_{rel} = 1.55 ± 0.09. The error bars represent the variance in 3 consecutive measurements. The uncertainty in k_{rel} corresponds to 3σ from the statistical analysis.

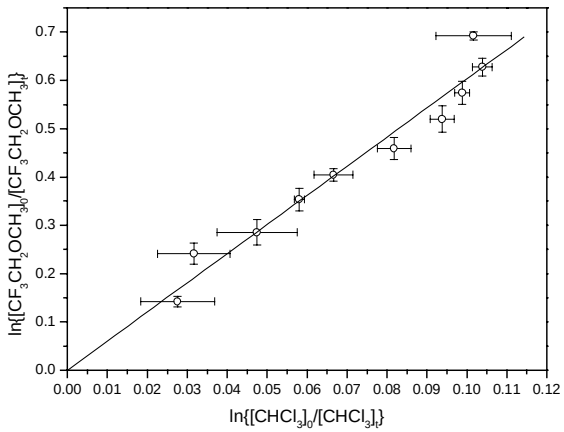

Fig. S2 Decay of $CF_3CH_2OCH_3$ versus $CHCl_3$ in the presence of OH radicals at 298 ± 2 K. 10 Data points give a relative reaction rate k_{rel} = 5.94 ± 0.31. The error bars represent the variance in 3 consecutive measurements. The uncertainty in k_{rel} corresponds to 3σ from the statistical analysis.

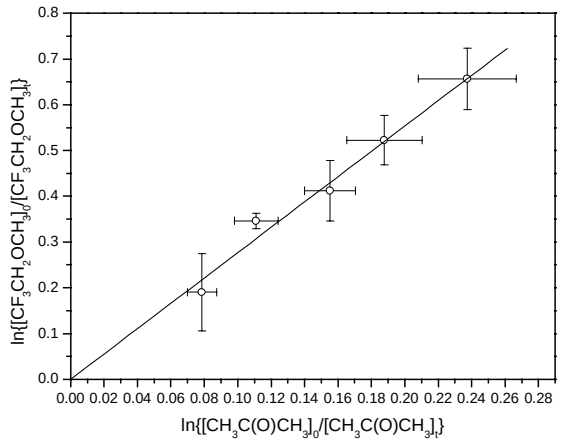

Fig. S3 Decay of $CF_3CH_2OCH_3$ versus $CH_3C(O)CH_3$ in the presence of OH radicals at 298 ± 2 K. 5 Data points give a relative reaction rate k_{rel} = 2.87 ± 0.30. The error bars represent the variance in 3 consecutive measurements. The uncertainty in k_{rel} corresponds to 3σ from the statistical analysis.

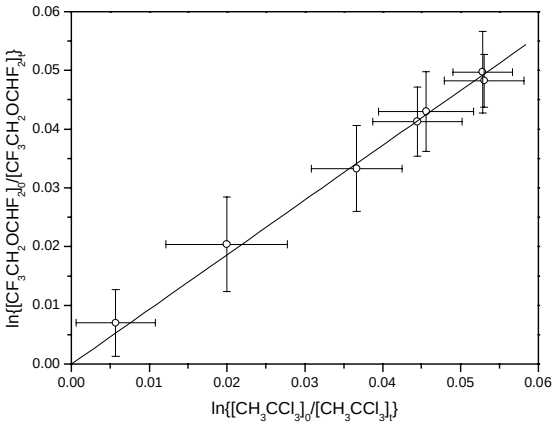

Fig. S4 Decay of $CF_3CH_2OCHF_2$ versus CH_3CCl_3 in the presence of OH radicals at 298 ± 2 K. 7 Data points give a relative reaction rate k_{rel} = 0.928 ± 0.032. The error bars represent the variance in 3 consecutive measurements. The uncertainty in k_{rel} corresponds to 3σ from the statistical analysis.

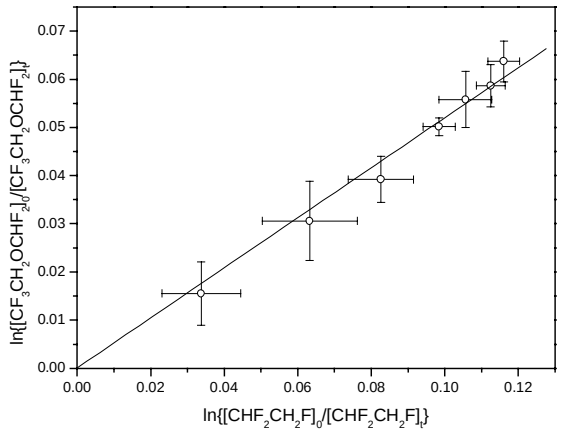

Fig. S5 Decay of $CF_3CH_2OCHF_2$ versus CHF_2CH_2F in the presence of OH radicals at 298 ± 2 K giving a relative reaction rate k_{rel} = 0.520 ± 0.024. The error bars represent the variance in 3 consecutive measurements. The uncertainty in k_{rel} corresponds to 3σ from the statistical analysis.

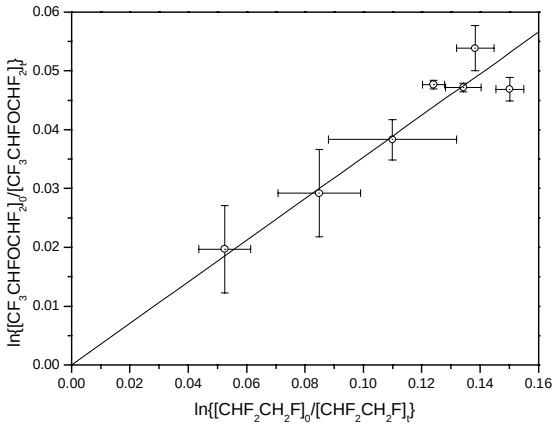

Fig. S6 Decay of $CF_3CHFOCHF_2$ versus CHF_2CH_2F in the presence of OH radicals at 298 ± 2 K. 7 Data points give a relative reaction rate k_{rel} = 0.36 ± 0.04. The error bars represent the variance in 3 consecutive measurements. The uncertainty in k_{rel} corresponds to 3σ from the statistical analysis.

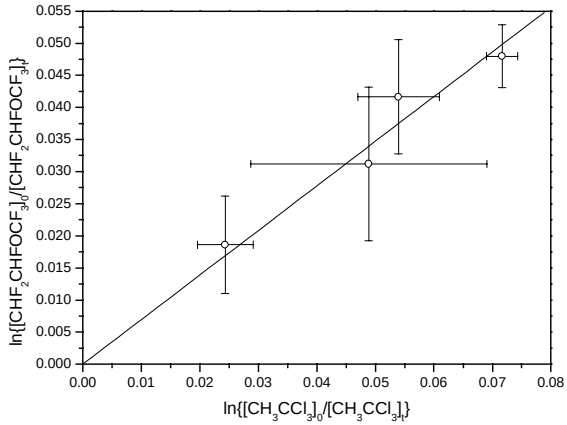

Fig. S7 Decay of $CHF_2CHFOCF_3$ versus CH_3CCl_3 in the presence of OH radicals at 298 ± 2 K. 4 Data points give a relative reaction rate k_{rel} = 0.69 ± 0.07. The error bars represent the variance in 3 consecutive measurements. The uncertainty in k_{rel} corresponds to 3σ from the statistical analysis.

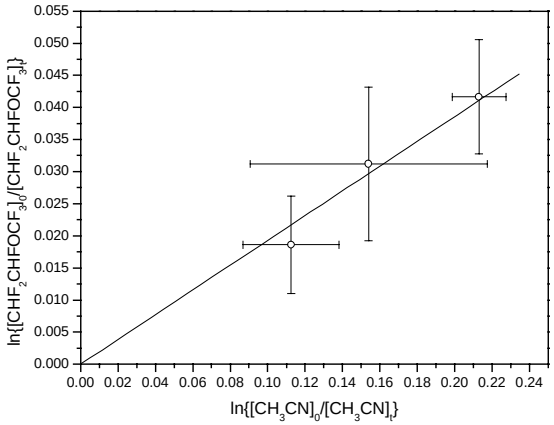

Fig. S8 Decay of $CHF_2CHFOCF_3$ versus CH_3CN in the presence of OH radicals at 298 ± 2 K. 3 Data points give a relative reaction rate k_{rel} = 0.229 ± 0.027. The error bars represent the variance in 3 consecutive measurements. The uncertainty in k_{rel} corresponds to 3σ from the statistical analysis.

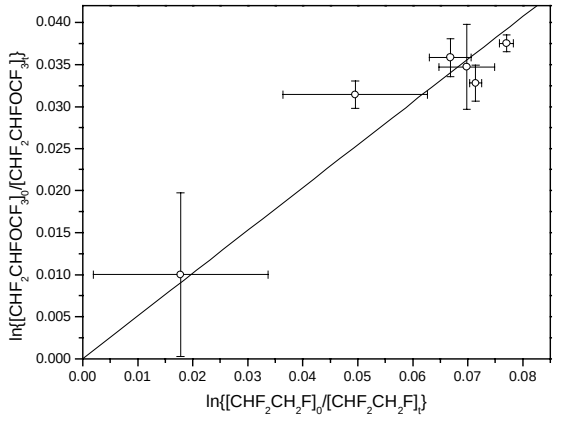

Fig. S9 Decay of $CHF_2CHFOCF_3$ versus CHF_2CH_2F in the presence of OH radicals at 298 ± 2 K. 6 Data points give a relative reaction rate k_{rel} = 0.487 ± 0.019. The error bars represent the variance in 3 consecutive measurements. The uncertainty in k_{rel} corresponds to 3σ from the statistical analysis.

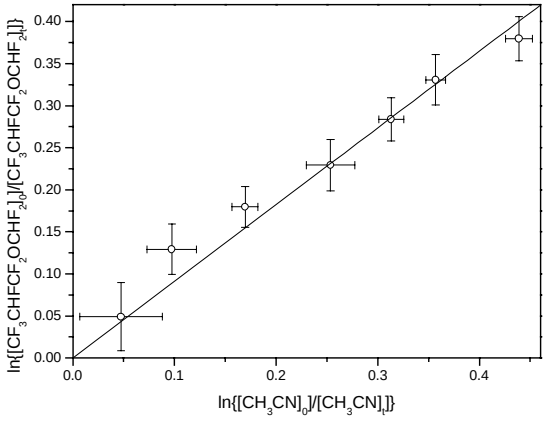

Fig. S10 Decay of $CF_3CHFCF_2OCHF_2$ versus CH_3CN in the presence of OH radicals at 298 ± 2 K. 7 Data points give a relative reaction rate k_{rel} = 0.91 ± 0.08. The error bars represent the variance in 3 consecutive measurements. The uncertainty in k_{rel} corresponds to 3σ from the statistical analysis.

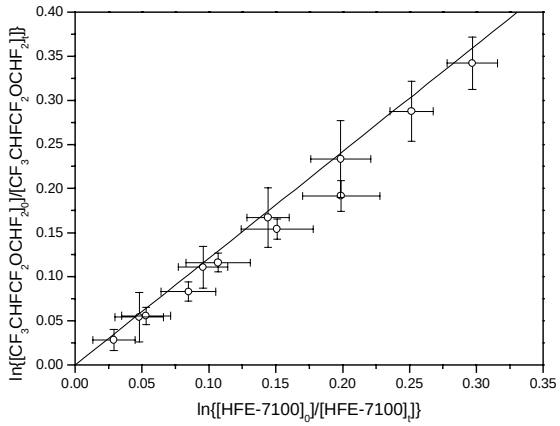

Fig. S11 Decay of $CF_3CHFCF_2OCHF_2$ versus $C_4F_9OCH_3$ (HFE-7100) in the presence of OH radicals at 298 ± 2 K. 12 Data points from 2 independent experiments give a relative reaction rate k_{rel} = 1.10 ± 0.07. The error bars represent the variance in 3 consecutive measurements. The uncertainty in k_{rel} corresponds to 3σ from the statistical analysis.

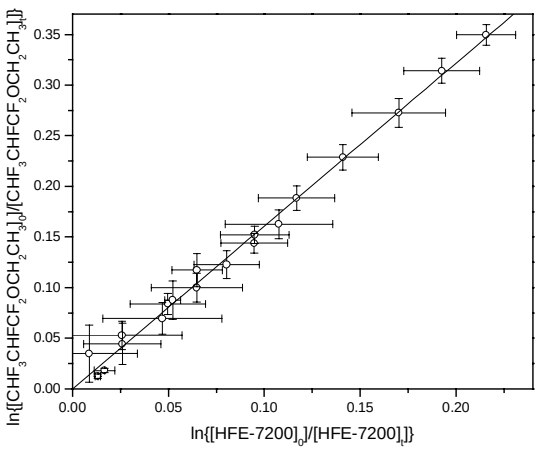

Fig. S12 Decay of $CF_3CHFCF_2OCH_2CH_3$ versus $C_4F_9OC_2H_5$ (HFE-7200) in the presence of OH radicals at 298 ± 2 K. 19 Data points from 2 independent experiments give a relative reaction rate k_{rel} = 1.69 ± 0.07. The error bars represent the variance in 3 consecutive measurements. The uncertainty in k_{rel} corresponds to 3σ from the statistical analysis.

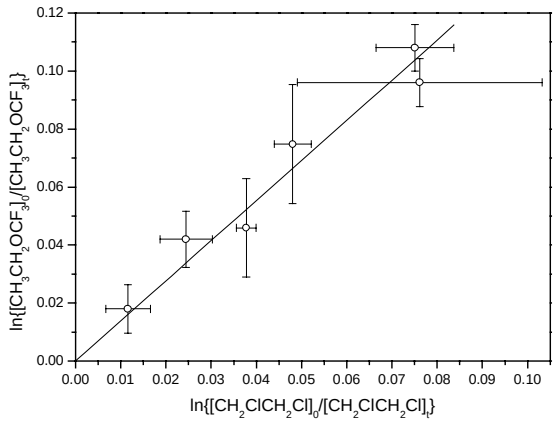

Fig. S13 Decay of $CH_3CH_2OCF_3$ versus CH_2ClCH_2Cl in the presence of Cl atoms at 298 ± 2 K. 6 Data points give a relative reaction rate k_{rel} = 1.44 ± 0.17. The error bars represent the variance in 3 consecutive measurements. The uncertainty in k_{rel} corresponds to 3σ from the statistical analysis.

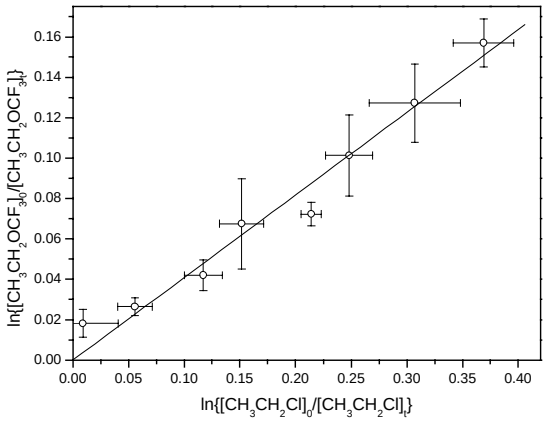

Fig. S14 Decay of $CH_3CH_2OCF_3$ versus CH_3CH_2Cl in the presence of Cl atoms at 298 ± 2 K. 8 Data points give a relative reaction rate k_{rel} = 0.38 ± 0.06. The error bars represent the variance in 3 consecutive measurements. The uncertainty in k_{rel} corresponds to 3σ from the statistical analysis.

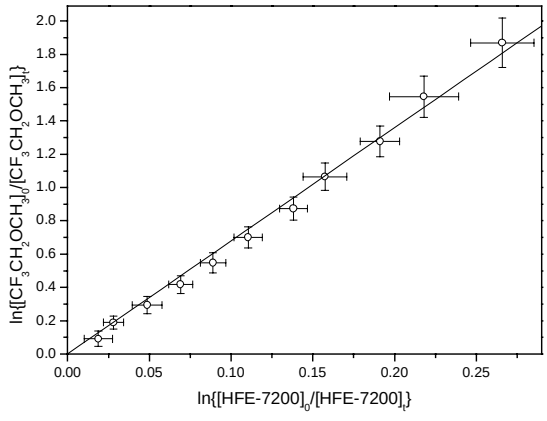

Fig. S15 Decay of $CF_3CH_2OCH_3$ versus $C_4F_9OC_2H_5$ (HFE-7200) in the presence of Cl atoms at 298 ± 2 K. 11 Data points give a relative reaction rate k_{rel} = 6.6 ± 0.4. The error bars represent the variance in 3 consecutive measurements. The uncertainty in k_{rel} corresponds to 3σ from the statistical analysis.

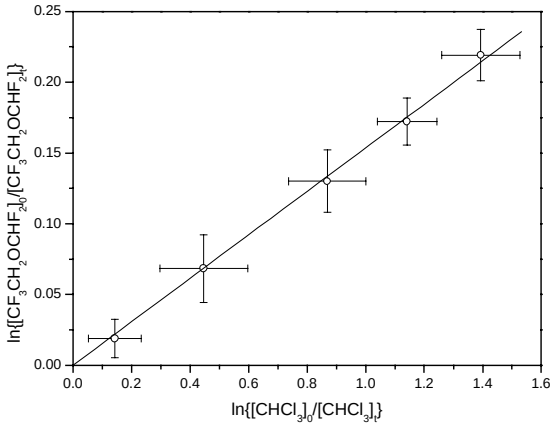

Fig. S16 Decay of $CF_3CH_2OCHF_2$ versus $CHCl_3$ in the presence of Cl atoms at 298 ± 2 K. 17 Data points from 2 independent experiments give a relative reaction rate k_{rel} = 0.153 ± 0.006. The error bars represent the variance in 3 consecutive measurements. The uncertainty in k_{rel} corresponds to 3σ from the statistical analysis.

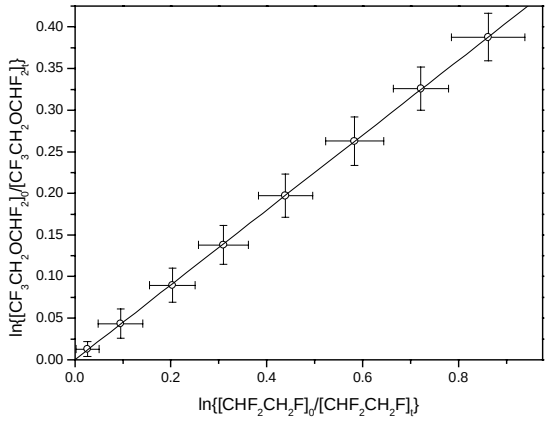

Fig. S17 Decay of $CF_3CH_2OCHF_2$ versus CHF_2CH_2F in the presence of Cl atoms at 298 ± 2 K. 17 Data points from 2 independent experiments give a relative reaction rate k_{rel} = 0.449 ± 0.004. The error bars represent the variance in 3 consecutive measurements. The uncertainty in k_{rel} corresponds to 3σ from the statistical analysis.

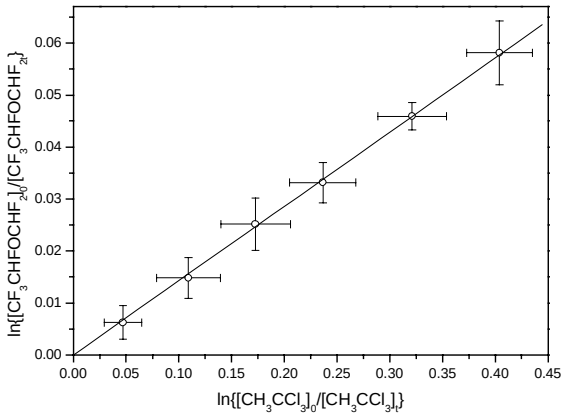

Fig. S18 Decay of $CF_3CHFOCHF_2$ versus CH_3CCl_3 in the presence of Cl atoms at 298 ± 2 K. 6 Data points give a relative reaction rate k_{rel} = 0.1426 ± 0.0031. The error bars represent the variance in 3 consecutive measurements. The uncertainty in k_{rel} corresponds to 3σ from the statistical analysis.

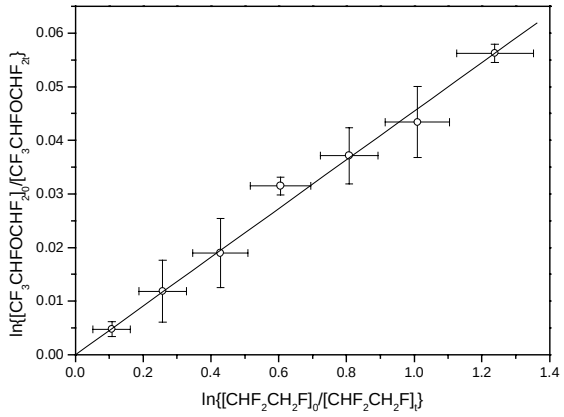

Fig. S19 Decay of $CF_3CHFOCHF_2$ versus CHF_2CH_2F in the presence of Cl atoms at 298 ± 2 K. 7 Data points give a relative reaction rate k_{rel} = 0.046 ± 0.004. The error bars represent the variance in 3 consecutive measurements. The uncertainty in k_{rel} corresponds to 3σ from the statistical analysis.

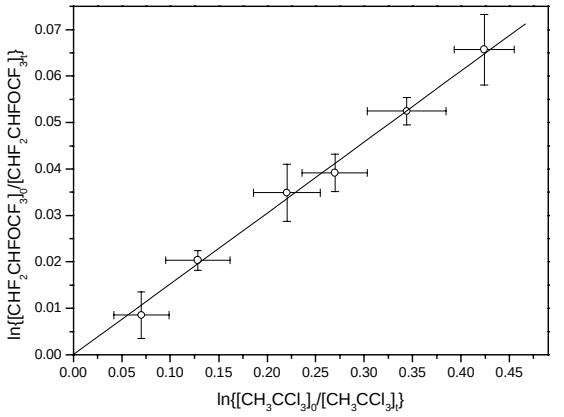

Fig. S20 Decay of $CHF_2CHFOCF_3$ versus CH_3CCl_3 in the presence of Cl atoms at 298 ± 2 K. 6 Data points give a relative reaction rate k_{rel} = 0.152 ± 0.008. The error bars represent the variance in 3 consecutive measurements. The uncertainty in k_{rel} corresponds to 3σ from the statistical analysis.

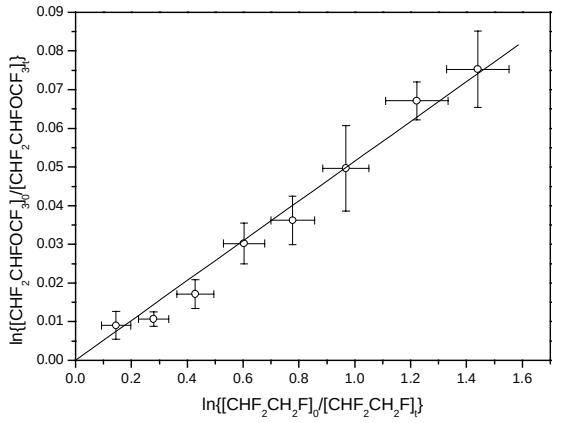

Fig. S21 Decay of $CHF_2CHFOCF_3$ versus CHF_2CH_2F in the presence of Cl atoms at 298 ± 2 K. 8 Data points give a relative reaction rate k_{rel} = 0.050 ± 0.07. The error bars represent the variance in 3 consecutive measurements. The uncertainty in k_{rel} corresponds to 3σ from the statistical analysis

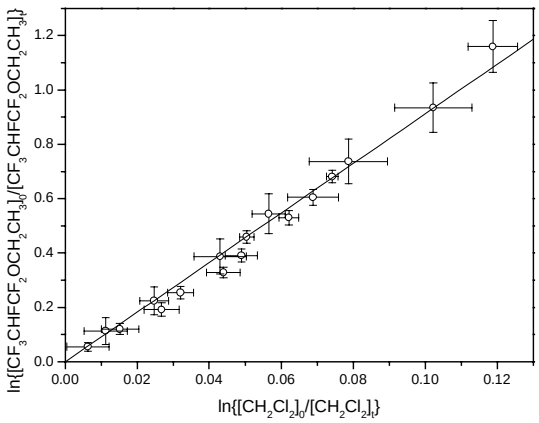

Fig. S22 Decay of $CF_3CHFCF_2OCH_2CH_3$ versus CH_2Cl_2 in the presence of Cl atoms at 298 ± 2 K. 17 Data points from 2 independent experiments give a relative reaction rate k_{rel} = 8.9 ± 0.4. The error bars represent the variance in 3 consecutive measurements. The uncertainty in k_{rel} corresponds to 3σ from the statistical analysis.

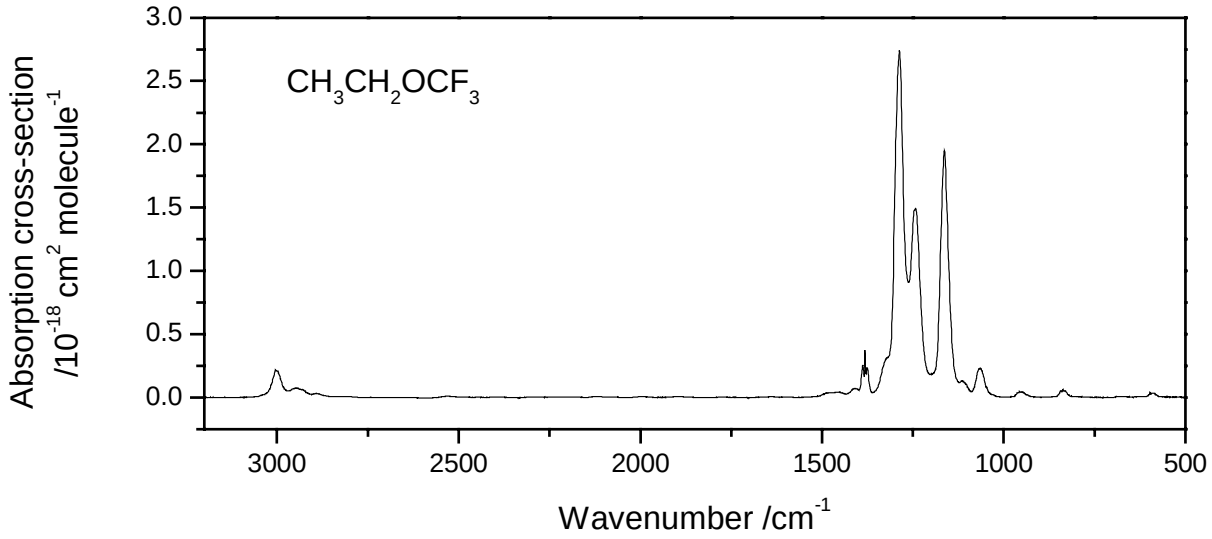

Fig. S23 Infrared absorption cross-section 3200-400 cm^{-1} (base e) of pure $CH_3CH_2OCF_3$ vapour at 298(2) K.

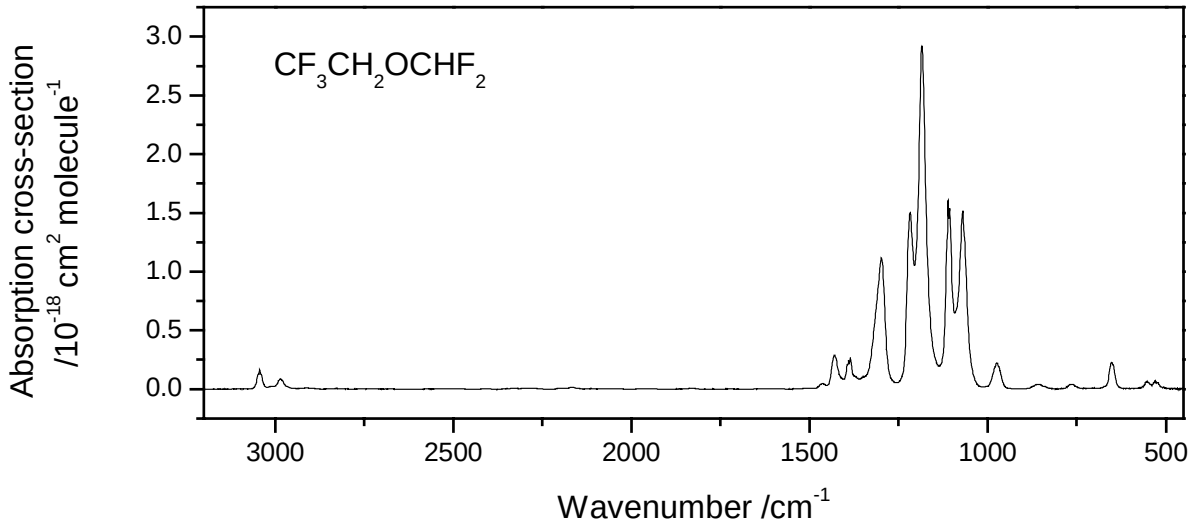

Fig. S24 Infrared absorption cross-section 3200-400 cm^{-1} (base e) of pure $CF_3CH_2OCHF_2$ vapour at 298(2) K.

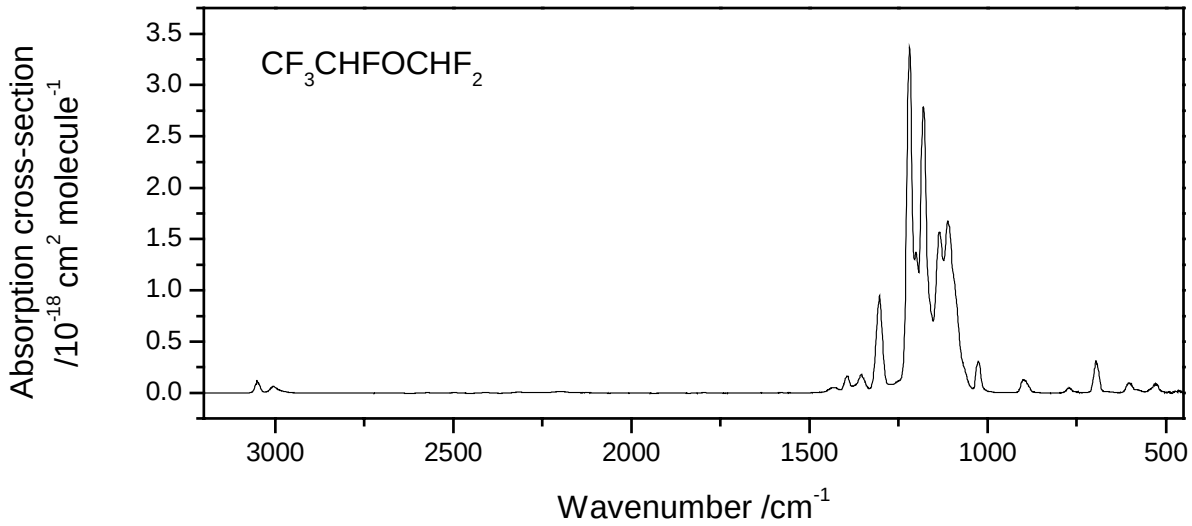

Fig. S25 Infrared absorption cross-section 3200-400 cm^{-1} (base e) of pure $CF_3CHFOCHF_2$ vapour at 298(2) K.

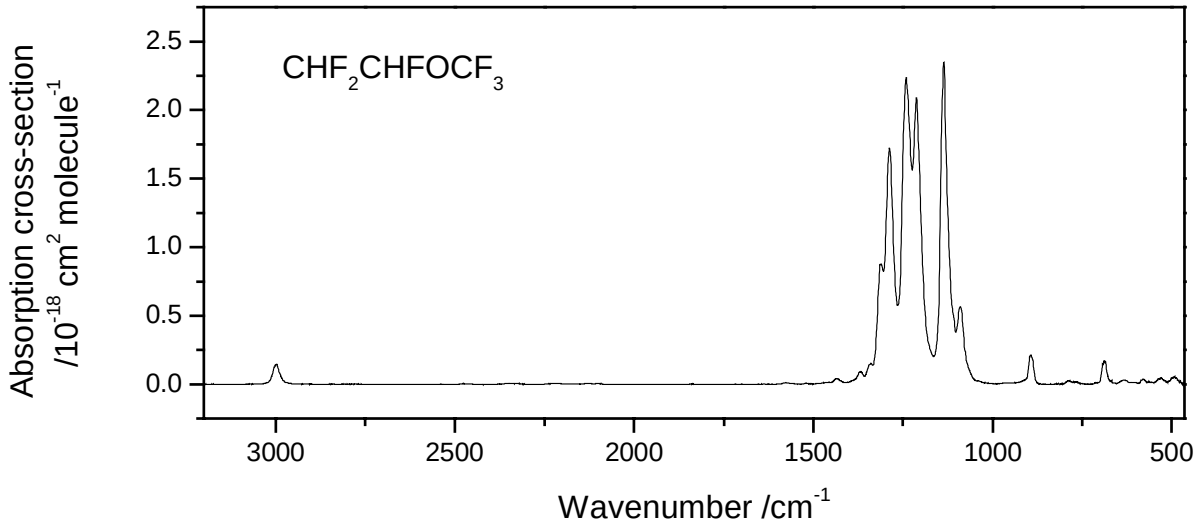

Fig. S26 Infrared absorption cross-section 3200-400 cm^{-1} (base e) of pure $CHF_2CHFOCF_3$ vapour at 298(2) K.

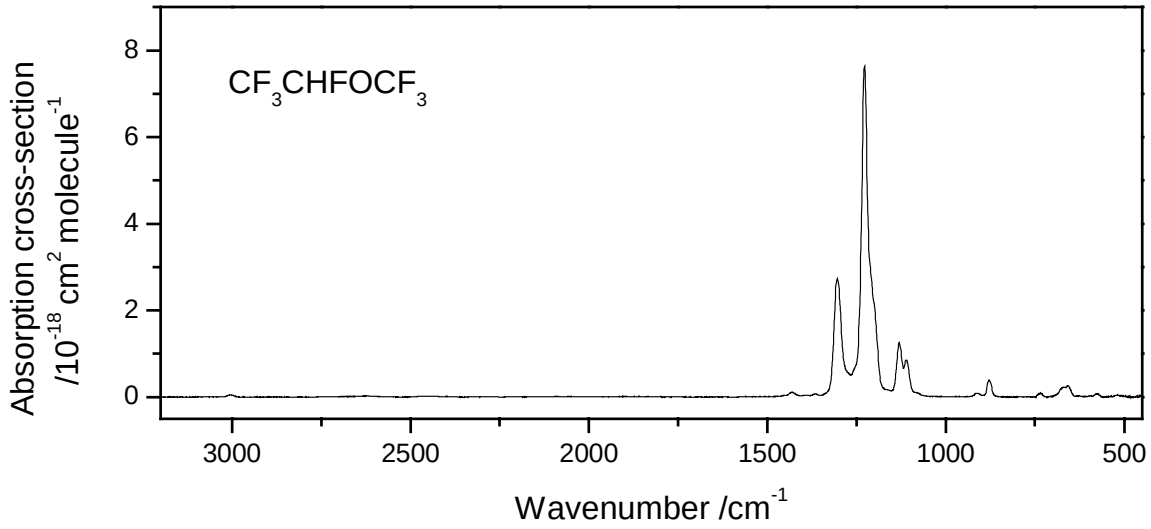

Fig. S27 Infrared absorption cross-section 3200-400 cm^{-1} (base e) of pure $CF_3CHFOCF_3$ vapour at 298(2) K.

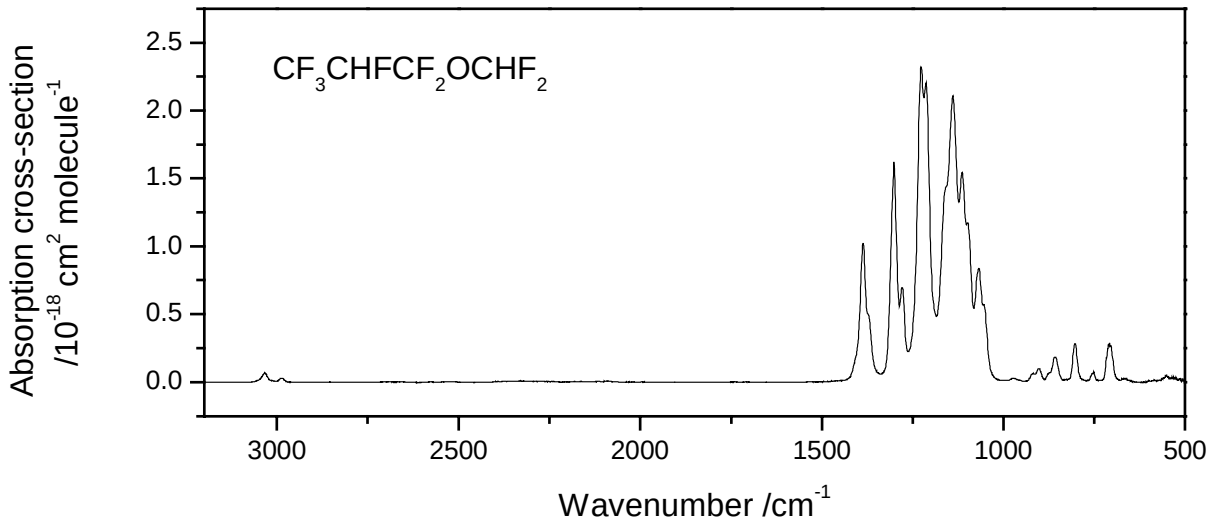

Fig. S28 Infrared absorption cross-section 3200-400 cm^{-1} (base e) of pure $CF_3CHFCF_2OCHF_2$ vapour at 298(2) K.

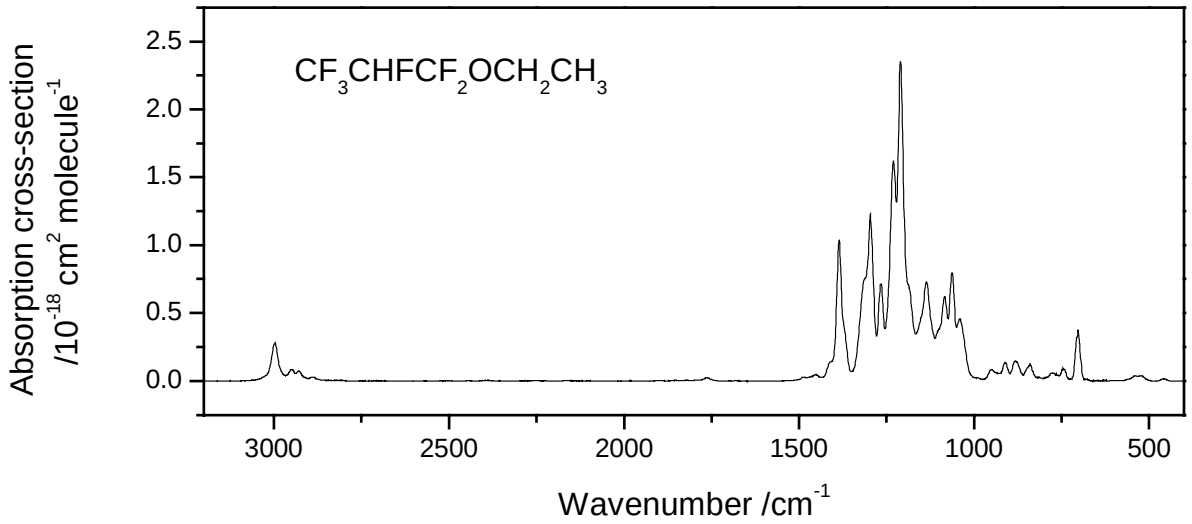

Fig. S29 Infrared absorption cross-section 3200-400 cm^{-1} (base e) of pure $CF_3CHFCF_2OCH_2CH_3$ vapour at 298(2) K.

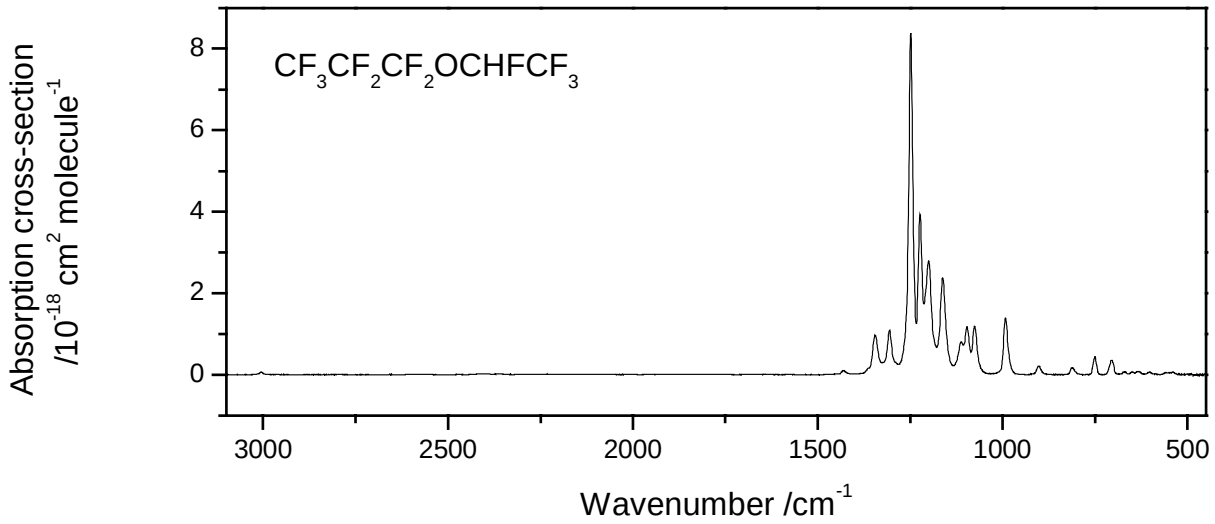

Fig. S30 Infrared absorption cross-section 3200-400 cm^{-1} (base e) of pure $CF_3CF_2CF_2OCHFCF_3$ vapour at 298(2) K.